

Supporting Information for “Arctic sea ice variability during the Instrumental Era”

M. Kathleen Brennan¹, Gregory J. Hakim¹, and Edward

Blanchard-Wrigglesworth¹,

¹Department of Atmospheric Sciences, University of Washington

Contents of this file

1. Data availability in Walsh et al 2017 (S1)
2. The early 20th century warming in reanalysis (S2)
3. Sensitivity of results (S3 – S5)
4. Verification Statistics (Equation 1)

1. Data availability in Walsh et al 2017

Walsh et al. (2017) uses sea ice observations from a ranked list of 12 different sources. When none of these observation types are available at a given time, temporal interpolation (for a single month of missing data) or analog based methods to fill in missing data (for periods with more than one month missing) are used. In Figure S1 we plot the percentage

Corresponding author: M. Kathleen Brennan, Department of Atmospheric Sciences, University of Washington, Seattle, WA, USA (mkb22@uw.edu)

of longitude ocean grid cells with an observation available for each month separated into two seasons from 1850–2013. The vertical green lines indicate April and September of 1953 respectively. Before March of 1953 there is very little spatial coverage of sea ice observations in the winter months (September–March). Data coverage in the summer months (April–August) is also very low (<40% on average) before May of 1901 and then returns to full coverage intermittently between 1902–1953.

2. The early 20th century warming in reanalysis

Figure S2 shows a comparison between annually averaged Arctic (north of 70N) mean temperature observations from HadCRUT and reanalysis data (NOAA-20C and ERA-20C) during the 20th century. Between 1953–2011 there is good agreement between HadCRUT and ERA-20C with an R^2 -value of 0.85 and R^2 -value of 0.41 between HadCRUT and NOAA-20C. In contrast before, 1953 these two records diverge with an R^2 -value of 0.27 and 0.01 respectively. Particularly from 1900–1953, ERA-20C temperature anomalies hover just below 0°C and NOAA-20C shows very cold anomalous temperatures of around -3°C, while HadCRUT increases from approximately -2°C to 1°C over the same time period. These discrepancies illustrate that neither of these reanalysis products capture the early 20th century warming.

3. Sensitivity of data assimilation results

Here, we quantify the sensitivity of our reconstructions to the choice of gridded temperature product assimilated (and their errors), climate model prior, and sample-error mediation in the DA (localization length scale and ensemble variance inflation factor).

3.1. Sensitivity to the observations

To test the sensitivity to the choice of assimilated observations, we assimilate three temperature products: HadCRUT, GISTEMP and Berkeley Earth (BE). The original temperature measurements used to create these products are mostly the same, and the main difference is the amount of interpolation (or infill) from grid cells with observations to grid cells with no observations for GISTEMP and BE. Reconstructions using all three temperature products are shown in Figure S3. The skill of the reconstruction during the satellite period is slightly higher when HadCRUT is assimilated, as measured by the R^2 values and coefficient of efficiency. Overall the source of the temperature observations has little effect on the overall variability of the reconstructions, with R^2 values with satellite data ranging from 0.82–0.89 for the MPI prior and 0.79–0.89 for the CCSM4 prior (described below). This is expected given the overall agreement among temperature products (e.g. (Rohde et al., 2013)).

For all of these experiments, an observed uncertainty of (\mathbf{R} in Equation 2) 0.4 K^2 is used for all three products as explained in the main manuscript. Other uncertainty estimates tested include: (1) using the annually averaged diagonal elements of the error covariance matrix provided with HadCRUT, and (2) using the variance across all three datasets at each point. Method (1) is ideal, but can only be applied to HadCRUT which has fewer data points than GISTEMP and BE because it does not use interpolation. For method (2) the variance across these datasets is very small, given that they often use the same original temperature observations. This led to an over-weighting of observations in the

Kalman gain and a SIE reconstruction with an inter-annual variability much larger than the satellite record.

3.2. Sensitivity to the prior

We use the MPI and CCSM4 Last Millennium simulations to test the sensitivity of the results to the choice of model prior. Figure S3 shows Arctic SIE from these two experiments (note that we use different inflation factors of 1.8 and 2.6 for the MPI and CCSM4 priors respectively, see below). Results show differences in inter-annual variability, but overall the decadal variability and the timing and magnitude of the ETCW are in close agreement (Figure S3). MPI-based reconstructions show slightly higher correlation with satellite data, with $R^2=0.82-0.89$, as compared to CCSM4-based reconstruction, with $R^2=0.79-0.89$.

3.3. Sensitivity to sample error: prior inflation and localization

The prior ensemble-perturbation inflation factor and prior spatial localization length scale are both determined empirically based on correlations with the trend in Arctic SIE in satellite observations, and correlation and coefficient of efficiency with satellite observations between 1979–2017. A series of experiments are performed with inflation factors ranging from 1.6–2.0 (incremented by 0.1) for the MPI prior and 2.3–2.7 (incremented by 0.1) for the CCSM4 prior. For each inflation factor, reconstructions are performed for localization radii of 5,000, 7,500, 10,000, 15,000, 20,000, and 25,000 km. As the basis of comparison, the trend, detrended variance, correlation and coefficient of efficiency with respect to satellite observations between 1979–2017 are determined across all iterations and ensemble members for each of the 30 parameter combinations (see Figure S4 and S5).

Increasing the localization length scale and the ensemble inflation of sea ice relative to temperature, both increase the temporal variance and trend in the reconstructions of SIE (Figures S4, S5). The results indicate that there is not only a trade-off between capturing the trend versus the inter-annual variability, but that there are various parameter combinations that show similar performance. Overall, all experiments described above using HadCRUT observations resulted in R^2 values greater than 0.86 and CE greater than 0.77 for MPI and R^2 values greater than 0.76 and CE greater than 0.62 for CCSM4.

4. Verification Statistics

To test the performance of our reconstructions we use both R^2 value (correlation coefficient squared) and coefficient of efficiency against satellite observations. The coefficient of efficiency (CE), like the correlation coefficient, measures the synchronicity in the variability of two datasets, but also quantifies mean bias and the difference in variance between the two datasets. This is a much stricter skill metric. Its maximum value is 1.0 and it is unbounded in the negative direction. A CE value of zero occurs when the sum of squared errors is equal to the variance in the verification data. Generally, positive CE values represent skill. It is defined as:

$$CE = 1 - \frac{\sum_i^n (v_i - x_i)^2}{\sum_i^n (v_i - \bar{v})^2}. \quad (1)$$

Here v is the verification value and x is the value being evaluated (the reconstructed value).

References

January 9, 2020, 3:47am

- Fetterer, F., Knowles, K., Meier, W. N., Savoie, M., & Windnagel, A. K. (2017). Sea Ice Index, Version 3. *NSIDC: National Snow and Ice Data Center, Boulder, Colorado USA*. doi: 10.7265/N5K072F8
- Rohde, R., Muller, R., Jacobsen, R., Perlmutter, S., & Mosher, S. (2013). Berkeley Earth Temperature Averaging Process. *Geoinformatics & Geostatistics: An Overview*, 01(02). doi: 10.4172/2327-4581.1000103
- Walsh, J. E., Fetterer, F., Scott Stewart, J., & Chapman, W. L. (2017, jan). A database for depicting Arctic sea ice variations back to 1850. *Geographical Review*, 107(1), 89–107. doi: 10.1111/j.1931-0846.2016.12195.x

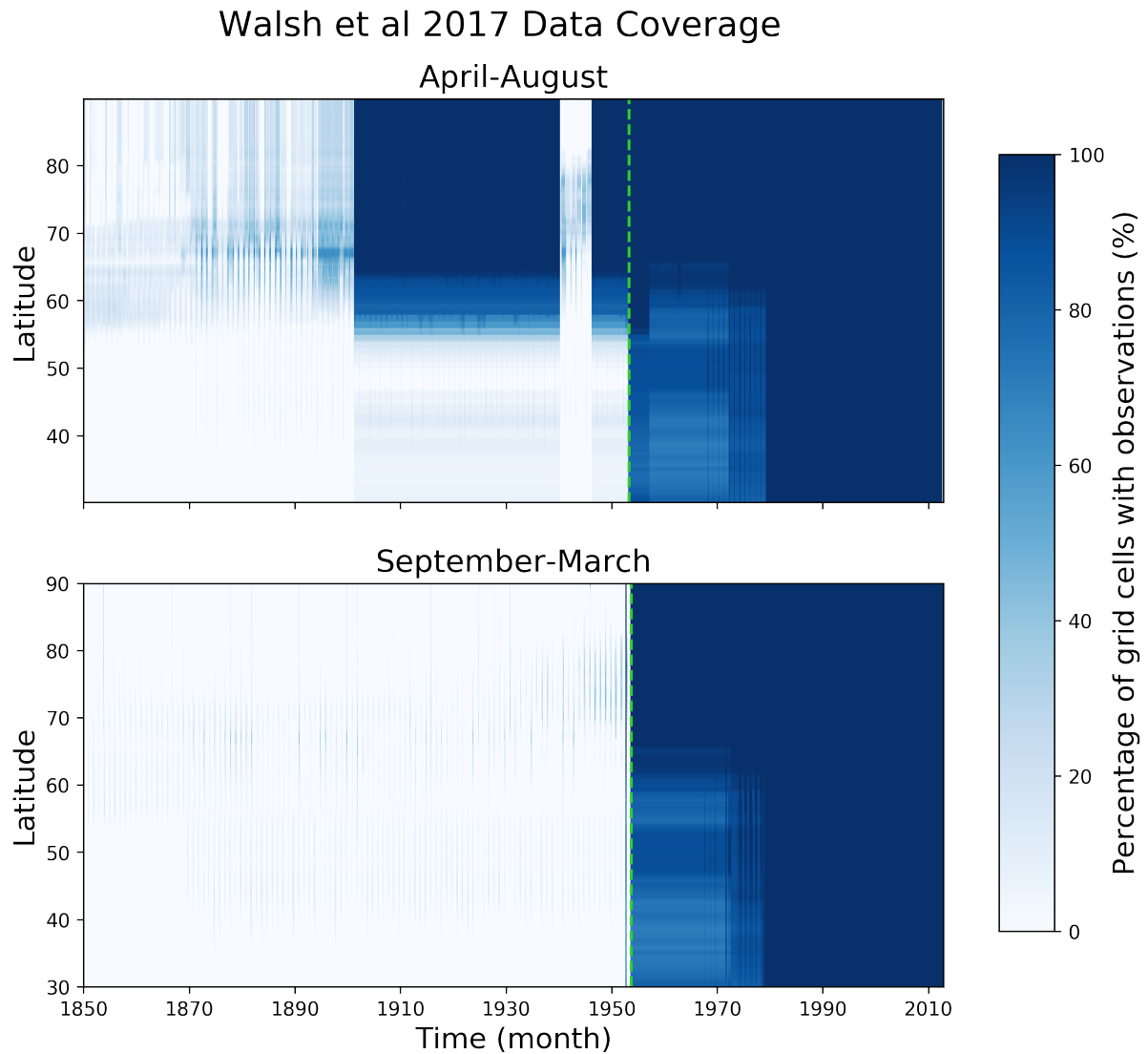


Figure S1. Shown is the data availability incorporated into the Walsh et al. (2017) Arctic sea ice record separated by two seasons over time. The color indicates the percentage of ocean longitude grid cells with an observation available at each latitude for each month. The vertical green lines indicate April 1953 and September 1953 respectively.

January 9, 2020, 3:47am

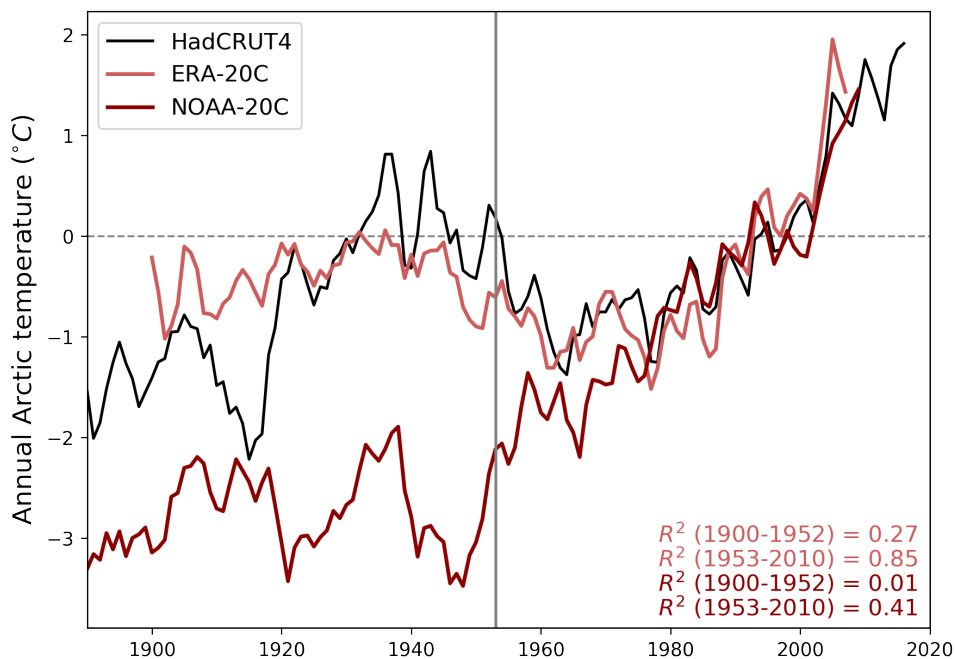


Figure S2. Arctic (north of 70N) mean surface air temperatures anomalies from HadCRUT, NOAA-20C, and ERA-20C. The vertical gray line indicates the year 1953, when availability of observations of sea ice in the Arctic decline substantially in the Walsh et al. (2017) record. Anomalies are centered about 1979-2011.

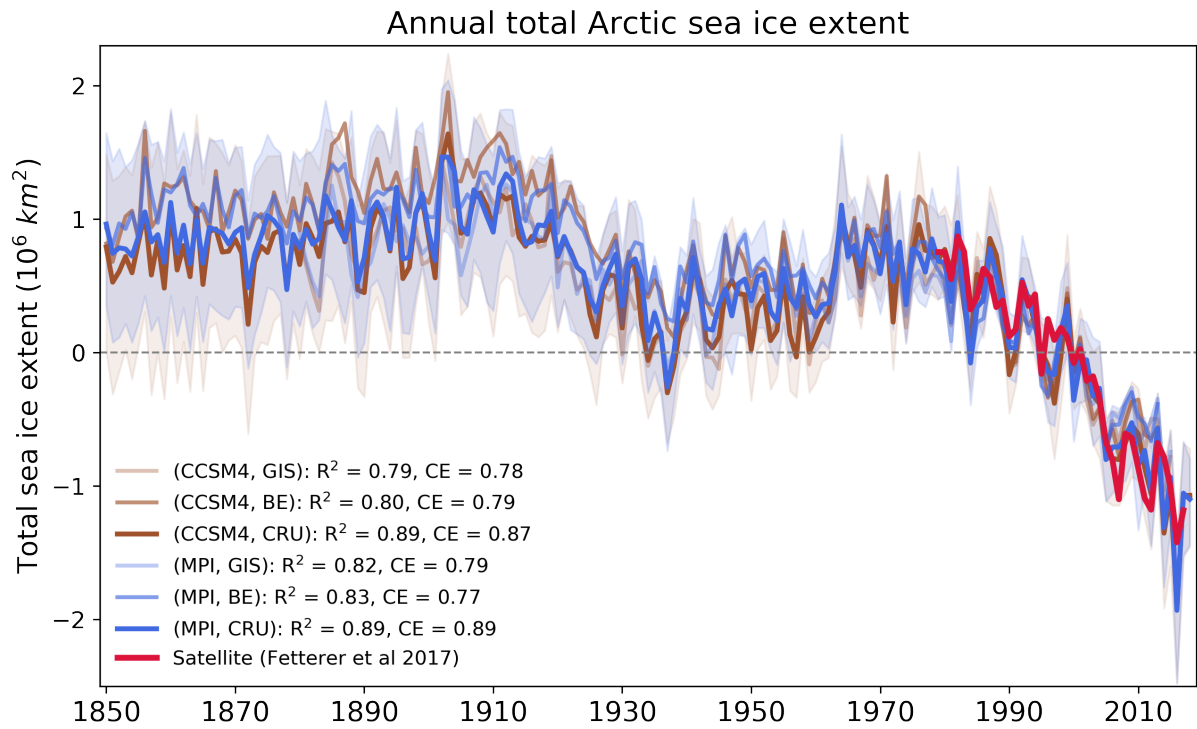


Figure S3. Total Arctic SIE reconstructed using priors drawn from two models (MPI and CCSM4 Last Millennium simulations) and three temperature datasets (HadCRUT, GISTEMP, and BE). For all experiments a localization length scale of 15,000 km is used and an inflation factor of 1.8 for MPI and 2.6 for CCSM4. The 97.5 and 2.5 percentiles of the ensemble spread are shown in blue and brown shading.

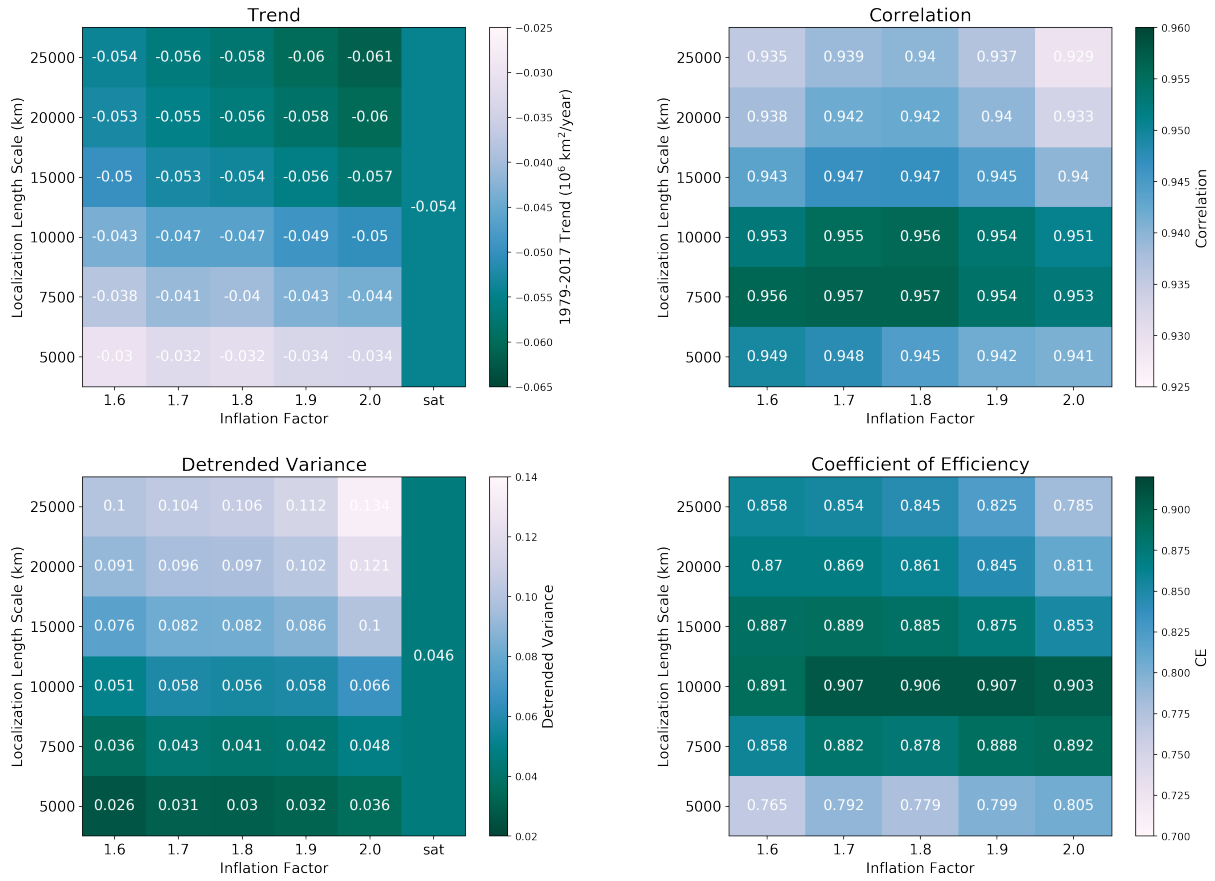


Figure S4. Verification statistics for 30 reconstructions performed using MPI as a model prior, HadCRUT observations, and different combinations of localization length scales (y-axis) and inflation factors (x-axis) are shown. Trends and detrended variances during the satellite era are shown in the two boxes on the left and the values observed in the satellite record (Fetterer et al., 2017) are shown in the column on the right. The correlation and coefficient of efficiency of these reconstructions when compared with (Fetterer et al., 2017) are shown in the two boxes on the right.

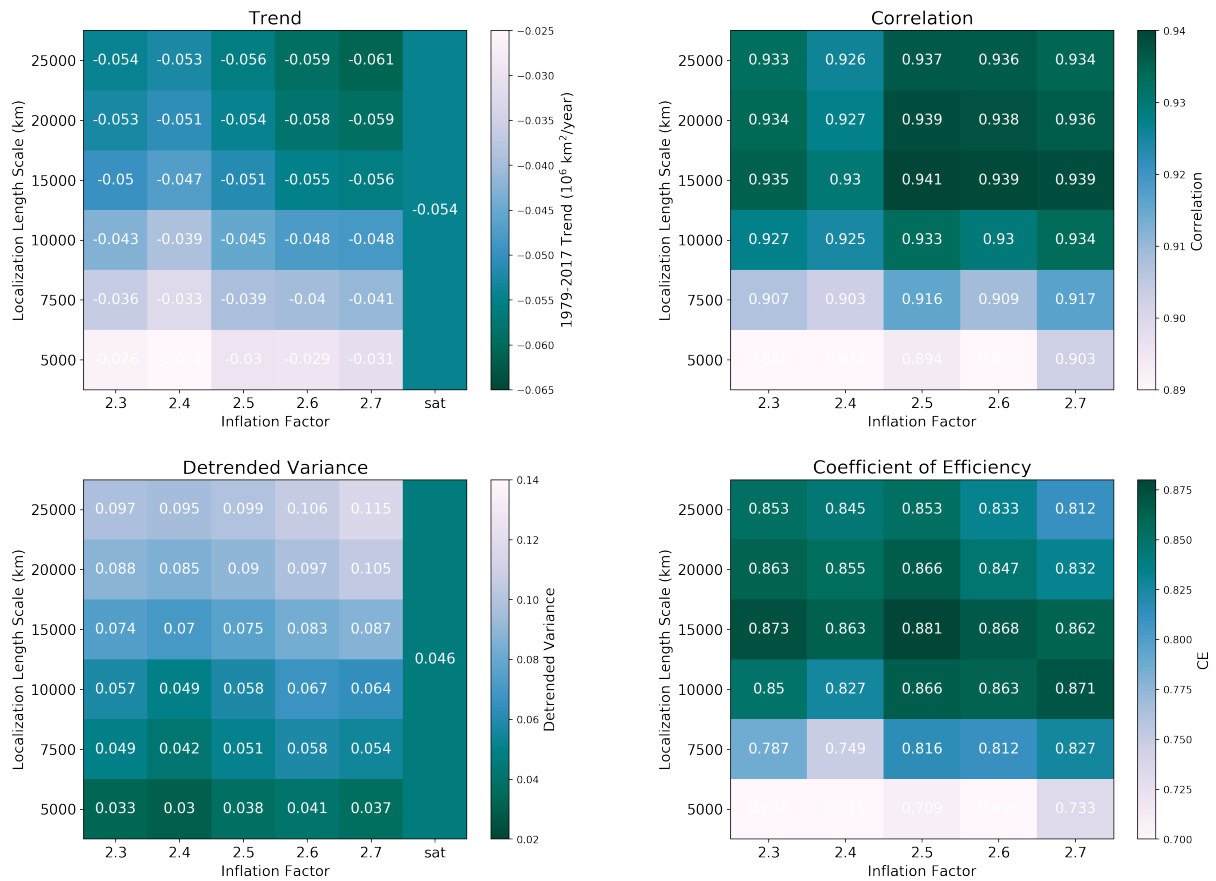


Figure S5. Verification statistics for 30 reconstructions performed using CCSM4 as a model prior, HadCRUT observations, and different combinations of localization length scales (y-axis) and inflation factors (x-axis) are shown. Trends and detrended variances during the satellite era are shown in the two boxes on the left and the values observed in the satellite record (Fetterer et al., 2017) are shown in the column on the right. The correlation and coefficient of efficiency of these reconstructions when compared with (Fetterer et al., 2017) are shown in the two boxes on the right.